REDUCING HALLUCINATIONS IN LARGE VISION-LANGUAGE MODELS VIA LATENT SPACE STEERING

Anonymous authors
Paper under double-blind review

ABSTRACT

Hallucination poses a challenge to the deployment of large vision-language models (LVLMs) in applications. Unlike in large language models (LLMs), hallucination in LVLMs often arises from misalignments between visual inputs and textual outputs. This paper investigates the underlying mechanisms of hallucination, focusing on the unique structure of LVLMs that distinguishes them from LLMs. We identify that hallucinations often arise from the sensitivity of text decoders to vision inputs, a natural phenomenon when image encoders and text decoders are pre-trained separately. Inspired by this, we introduce Visual and Textual Intervention (VTI), a novel technique designed to reduce hallucinations by steering latent space representations during inference to enhance the stability of vision features. As a task-agnostic test-time intervention, VTI can be easily applied to any problem without additional training cost. Extensive experiments demonstrate that it can effectively reduce hallucinations and outperform baseline methods across multiple metrics, highlighting the critical role of vision feature stability in LVLMs.

1 INTRODUCTION

Large Vision-Language Models (LVLMs) (Liu et al., 2023b; Zhu et al., 2023; Ye et al., 2023; Li et al., 2023a; Dai et al., 2023; Gong et al., 2023; Bai et al., 2023b) have demonstrated impressive performance across various tasks such as image captioning (Li et al., 2023b; Wang et al., 2023b), visual question answering (Lee et al., 2024; Wang et al., 2024a), medical treatment planning (Liu et al., 2024b), and many more. LVLMs take advantage of both powerful vision encoders such as CLIP (Radford et al., 2021) and text decoders, which are often pretrained large language models, and can present sophisticated understanding of vision information by mapping them to the language domain where LLMs can process.

Despite their remarkable success, LVLMs still encounter numerous challenges that impede their applications in real-world tasks, among which hallucination (Liu et al., 2023a; Lovenia et al., 2023; Leng et al., 2023b; Liu et al., 2024a; Deng et al., 2024; Zhu et al., 2024) is one prominent concern (Gunjal et al., 2023; Li et al., 2023c). Hallucination in LVLMs emerges when the generated textual responses include inaccurate descriptions of the input image (Li et al., 2023c), such as mentioning non-existing objects or characters, or providing incorrect spatial relations. Such kind of cross-modality inconsistency arises from a different mechanism from that in standard LLMs, where vision information is missing and hallucination comes solely from the linguistics level. In LVLMs, the sequential relation of information flow from the vision encoder to the text decoder can distinctly contribute to hallucination, a potentially essential question to be answered.

While a few existing studies have explored the underlying mechanism in this regard, leading to different conclusions such as statistical pre-training bias (Agarwal et al., 2020; Agrawal et al., 2016; Goyal et al., 2017), over-reliance on language prior (Leng et al., 2023b; Lee et al., 2023; Zhibo et al., 2023; Han et al., 2022; Wu et al., 2022), and biased feature learning (Zhu et al., 2024; Huang et al., 2023; Yue et al., 2024), they focus mainly on issues that do not distinguish between LVLMs and LLMs. That is, the mechanisms of hallucination they present do not take into consideration the particular structure of LVLMs that differs from LLMs.

This paper explores the mechanism of hallucination based on the sequential relation from vision encoder to the text decoder: we demonstrate that hallucinations can stem from the sensitivity to the unstability of the vision encoders. Similar to conventional neural networks in computer vision, an

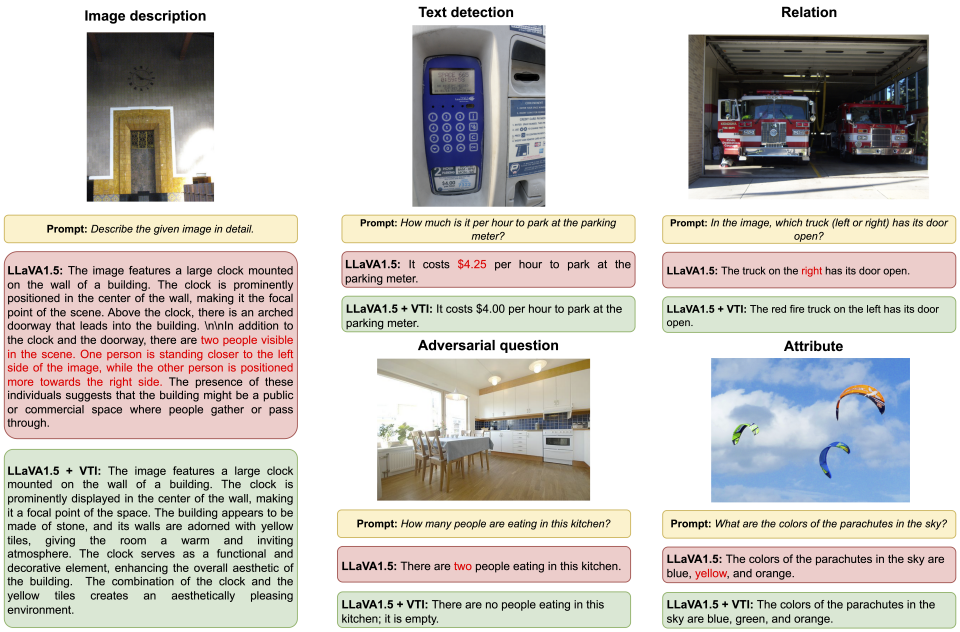

Figure 1: Illustration of the effect of our proposed method, VTI, using LLaVA-1.5. Hallucinated contents generated by the original model are marked in red. In contrast, VTI results in less hallucination across different categories of questions. Examples are obtained from MMHAL-Bench (Sun et al., 2023) and CHAIR (Rohrbach et al., 2018)

ideal vision encoder should output stable features when the semantics of images remain unchanged, e.g., after we perturb them mildly. This is especially the case for LVLMs where the image encoder and the text decoder are pre-trained separately and minimally fine-tuned together. The sensitivity of the text decoder to image features can exacerbate the misalignment between both modalities and results in hallucinations. We comprehensively present and analyze the correlation between vision feature stability and model hallucinations in Section 3.

A naive way to reduce model hallucination is to smooth vision features by averaging across multiple perturbations of the original image every time we have a new query. Unfortunately, this not only requires multiple forward pass of the model which is extremely inefficient but also introduce extra noises to the original features, leading to worse preservation of information. To better leverage the correlation and reduce hallucinations without introducing additional side effects, inspired by works on representation engineering for LLMs (Liu et al.; Cao et al., 2024; Luo et al., 2024; Zou et al., 2023), where LLM's behavior is altered by editing the latent features, we pre-compute the direction that feature averaging has brought in the latent space and apply them to edit the latent features of any new query. The pre-computed directions in the latent space capture the underlying changes as we perturb the query image and average vision embeddings across perturbations. This simple yet effective test-time intervention on vision, when combined with intervetion on text, allows our proposed method, namely **Visual and Textual Intervention** (VTI), to mitigate vision-language hallucinations. Importantly, we use a fixed 50 examples to pre-compute all intervention directions, and applied consistently across all benchmarks, suggesting VTI is task and dataset agnostic.

In summary, we (1) investigate the mechanism of hallucination by focusing on the sequential relationship between the vision encoder and text decoder, uncovering a correlation between the stability of visual features and hallucinations of LVLMs, (2) propose a novel method, VTI, which guides LVLMs toward less hallucinated outputs by steering them in the latent space, and (3) conduct extensive experiments to benchmark VTI against baseline methods. The leading results across multiple metrics demonstrate the high effectiveness of VTI in reducing hallucinations. We hope that our work can shed light on the critical role of feature stability in LVLMs and inspire future research to develop more effective strategies for reducing hallucinations.

2 RELATED WORK

Large Vision-Language Models. The success of Large Language Models (LLMs)(Gilardi et al., 2023; Touvron et al., 2023; Tay et al., 2022; Raffel et al., 2020; Brown et al., 2020; Chowdhery et al., 2022; Taori et al., 2023; Chiang et al., 2023; Bai et al., 2023a) has fueled significant advancements in Large Vision-Language Models (LVLMs)(Liu et al., 2023b; Dai et al., 2023; Zhu et al., 2023; Li et al., 2023a; Ye et al., 2023; Bai et al., 2023b). By incorporating visual encoders and feature projectors (Li et al., 2019; Sun et al., 2019; Wang et al., 2022; Li et al., 2022), LVLMs have achieved notable improvements across a variety of multimodal tasks, including image captioning (Li et al., 2023b), visual question answering (Zhang et al., 2023a), and image segmentation (Lai et al., 2024). However, similar to LLMs, LVLMs are susceptible to generating hallucinations (Li et al., 2023c), which hinder their robustness and reliability in real-world applications. Our work seeks to address this by mitigating hallucinations in LVLMs, thereby enhancing their utility and dependability in practical settings.

Hallucination in Vision-Language Models and LVLMs. In natural language processing, hallucination refers to the generation of false or nonsensical content (Ji et al., 2023; Zhang et al., 2023b; Shi et al., 2023). This issue has recently drawn attention in multimodal models, where hallucinations can significantly impair performance (Wang et al., 2023a; Zhao et al., 2023; Huang et al., 2023; Yue et al., 2024). To counter this, various methods have been proposed, primarily involving additional training to align models with ground truth (Gunjal et al., 2023; Liu et al., 2023a; Sun et al., 2023; Yin et al., 2023; Zhou et al., 2023; Zhai et al., 2023; Yue et al., 2024). However, such approaches often suffer from practical limitations, such as the need for extensive training and additional data. In response, training-free methods have gained traction. These approaches rely on techniques like self-feedback correction (Lee et al., 2023; Yin et al., 2023), leveraging auxiliary models for knowledge integration (Wan et al., 2024; Deng et al., 2024; Zhao et al., 2024; Yang et al., 2024; Kim et al., 2024), and refining the model's decoding process (Huang et al., 2023; Leng et al., 2023a; Favero et al., 2024; Zhang et al., 2024; Wang et al., 2024b). These methods typically focus on adjusting the text decoder but are limited in addressing hallucinations originating from visual components.

In contrast, our approach targets hallucination reduction by directly steering the latent feature space, impacting both the vision encoder and text decoder. This strategy enables us to mitigate hallucinations arising from both vision and text-centric sources, making our method more comprehensive than those focused solely on refining the text output.

3 MECHANISM OF HALLUCINATION IN LVLMS

A large vision language model typically consists of a vision encoder and a large language model as a text decoder. Given an image v, a text input x such as a question or prompt about the image, the vision encoder first extracts visual information from the image as vision feature vectors $V = \{v_1, v_2, \ldots, v_n\}$. These vision features are then projected into the same embedding space as the text input, and both the vision and text embeddings are concatenated and passed to the text decoder to generate text outputs auto-regressively. While LVLMs are known to hallucinate, the underlying causes of this phenomenon remain unclear, particularly in relation to the vision encoder's role in the process. In this section, we explore how the stability of vision features impacts hallucination.

We begin by highlighting a fundamental relationship between the vision and text components of large vision-language models: the output of the vision encoder serves as the input to the language decoder. This sequential connection implies that the stability of the vision features plays a crucial role in the model's outputs and can influence the occurrence of hallucinations. To examine the connection between feature stability and object hallucination, we perturb raw images with various types of noise and analyze the variance in the resulting feature distributions. Ideally, noise that does not alter an image's semantic content should have minimal impact on the vision features or the model's output, provided the vision encoder is robust and trained to capture semantic information effectively.

However, as shown in the left figure of Figure 2, while most vision features remain stable, approximately 15% exhibit significant variance, resulting in a long-tailed distribution. These unstable features are closely tied to hallucinations, as the model becomes overly sensitive to these features, leading to inaccuracies in its outputs.This connection is further demonstrated in the second figure

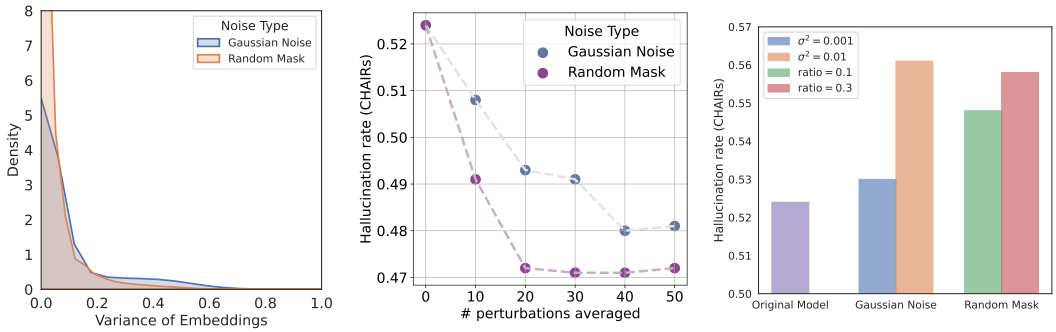

Figure 2: (Left) Distribution of vision feature stability when different types of noise are injected into the raw images. The x-axis represents the variance of features across 50 perturbations, and the y-axis represents the frequency. (Middle) Illustration of the correlation between object hallucination and vision feature stability. Averaging vision features across multiple perturbed images reduces hallucination (measured by CHAIR, details in Section A) as the number of perturbations averaged increases. (Right) Noise alone tends to increase hallucination, suggesting that the reduction of hallucination is not due to the noise itself but to the averaging process across perturbations.

of Figure 2: averaging vision features across multiple noise-injected images reduces hallucination as the number of perturbations increases, regardless of the type of noise injected. Importantly, as shown in the right figure, this reduction is not due to the noise itself but to the averaging process across perturbations, while noise alone tends to increase hallucination.

Although feature averaging can mitigate hallucination, it introduces significant drawbacks. Since vision encoders are trained on clean data, perturbing images compromises information extraction, leading to a loss of detail. Moreover, averaging vision features requires multiple forward passes through the model, greatly increasing computational costs. Thus, our goal is to develop a method that enhances vision feature stability and reduces hallucination efficiently, without sacrificing information or incurring excessive computational overhead.

4 METHOD

The experiments in the previous section demonstrate that features averaged across mildly corrupted images are robust and effective in reducing hallucinations, despite the side effects. To avoid this, inspired by works on representation engineering for LLMs (Liu et al.; Cao et al., 2024; Luo et al., 2024; Zou et al., 2023), where LLM's behavior is altered by editing the features in the latent space during inference, we develop a computationally efficient algorithm called **visual and textual intervention** (VTI) that can improve vision feature stability as well as text to image dependancy to reduce hallucination of LVLMs. In particular, we pre-compute the "direction" of more stable features and then apply them consistently to all query examples during inference to reduce hallucination, without introducing additional training or inference cost. As sometimes hallucination rise from the text decoder, i.e. the LLM, we further obtain a textual direction and apply it to the text decoder to maximize the performance. The overview of the proposed method is illustrated in Figure 3.

Given a vision input v, let the latent states of the vision encoder for v be represented as $h^v_{l,t}$, where $l \in \{1, 2, \ldots, L\}$ denotes the layer index in the encoder, and $t \in \{1, 2, \ldots, T\}$ represents the index of the vision tokens.

To enhance the robustness of the latent representation, we leverage random masking to create multiple perturbed versions of v. Specifically, we apply m different random masks, $\mathcal{C}_i,\ i = 1, \ldots, m$, to v, producing m corrupted versions, $\mathcal{C}_i(v)$. For each perturbed input $\mathcal{C}_i(v)$, the vision encoder generates the corresponding latent states $h^{\mathcal{C}_i(v)}_{l,t}$.

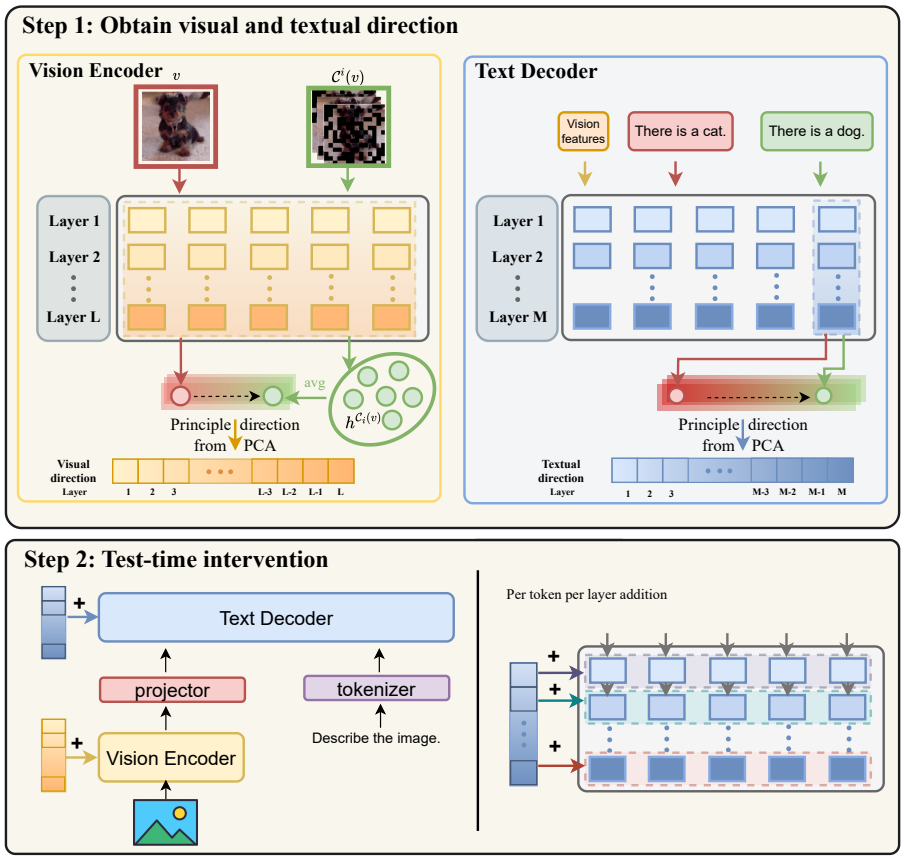

Figure 3: Overview of the proposed algorithm visual and textual test-time intervention (VTI). Given a example set $\{(v_i, x_i, \tilde{x}_i)\}_{i=1}^N$ where v_i is the vision input and $(x_i, \tilde{x}_i)$ is paired captions with and without hallucination, VTI first runs the model on each query $(v_i, x_i, \tilde{x}_i)$ and records all hidden states. It then computes the shifting vectors $d_{l,t}^{\text{vision}}$ and $d_{l,t}^{\text{text}}$ for all layer l and token t according to Section 4. During inference, the vectors are subsequently added to every layer of the vision encoder and text decoder, respectively, when processing a new query. Notice that the vectors are task- and dataset-agnostic, i.e., they are pre-computed using a few samples from one specific task and dataset, and fixed unchanged throughout the entire experiments in our paper.

Intuitively, a robust latent embedding for v can be approximated by averaging the embeddings obtained from the perturbed inputs. This averaged embedding is computed as:

$$\bar{h}_{l,t}^{v} = \frac{1}{m} \sum_{i=1}^{m} h_{l,t}^{\mathcal{C}_i(v)}.$$

The **visual shifting vector** is then defined as the difference between the robust averaged embedding and the original embedding:

$$\Delta_{l,t}^{v} = \bar{h}_{l,t}^{v} - h_{l,t}^{v}. \tag{1}$$

To make this shifting vector applicable to new image queries, we aim to remove image-specific information from $\Delta_{l,t}^{v}$, retaining only the general effect introduced by feature averaging. To achieve this, we compute the shifting vectors $\Delta_{l,t}^{v_i}$ for a set of N example images, $\{v_1, v_2, \ldots, v_N\}$. By stacking these vectors into a matrix,

$$[\Delta_{l,t}^{v_1}, \Delta_{l,t}^{v_2}, \ldots, \Delta_{l,t}^{v_N}],$$

we extract the first principal direction of this matrix, denoted as $d_{l,t}^{\text{vision}}$. This principal direction captures the dominant pattern of change introduced by feature averaging (an ablation study of the PCA dimensions is provided in Table 5).

It is worth noting that for each image, the random mask applied to generate the perturbed inputs $\mathcal{C}_i(v)$ is independently sampled, ensuring diversity in the perturbations and improving the generality of the computed shifting vector.

Apart from the vision token shifting, we further introduce the textual shifting vector that steers the latent states of the text decoder when generating model outputs. Obtaining the textual shifting vector is as simple as what previous work proposed in aligning the style of LLMs; Following (Zhou et al., 2023), we curated N image captions without hallucination, denoted as x and adopt GPT model generate the hallucinated version $\tilde{x}$. As a result, we obtain paired captions with and without hallucination. We simply use the original corresponding images v as the visual inputs. We then compute the textual direction for each of the sample as

$$\Delta_{l,t}^{x_i,v_i} = h_{l,t}^{x_i,v_i} - h_{l,t}^{\tilde{x}_i,v_i}, \tag{2}$$

where $h_{l,t}$ stands for the hidden states of the t-th text token in layer l when generating the last token of outputs. In particular, since the text decoder is causally modeled, we only use latent states of the last token, i.e. $t =$ the last token. Similarly, we perform PCA to remove extra noise from a specific example choice to obtain the overall direction $d_{l,t}^{\text{text}}$.

We separately apply the visual and textual direction to Intervene vision encoder and the text decoer, i.e. the LLM. Since the vision encoder is not causally modeled, we shift the latent states of all layers of the vision encoder at all token positions in the forward pass:

$$h_{l,t}^{v} := h_{l,t}^{v} + \alpha \cdot d_{l,t}^{\text{vision}}, \tag{3}$$

and for the text, we shift the latent states of the text decoder with the textual direction:

$$h_{l,t}^{x,v} := h_{l,t}^{x,v} + \beta \cdot d_{l,t=\text{last token}}^{\text{text}}, \tag{4}$$

As we will demonstrate in the experimental section below, such a combination of vision and language latent space intervention can address various styles of hallucination.

5 Experiments

In this section, we empirically investigate the effectiveness of VTI in reducing hallucinations. Remarkably, we use 50 examples with paired images (from COCO (Lin et al., 2014)), hallucinated and non-hallucinated responses to pre-computed the visual and textual direction and apply them to all tasks, datasets, and queries. This ensures the universality and generalizability of our results. We aim to answer the following questions: (1) Can visual intervention effectively reduce hallucination in LVLMs? (2) Can textual intervention effectively reduce hallucinations in LVLMs? (3) What is the benefit of combining them?

5.1 Experimental Settings

Datasets. We evaluate our model on both discriminative and generative datasets as listed below. More details about the datasets are provided in the appendix. **(a) POPE**: The Polling-based Object Probing Evaluation (Li et al., 2023c) contains 27,000 Yes/No questions about object existence in MSCOCO (Lin et al., 2014), where the task is to judge whether the given object is in the given image (examples are provided in Figure 7). Following existing works, we compute accuracy, precision, recall, and F1 score for each method. **(b) CHAIR**: Caption Hallucination Assessment with Image Relevance (Rohrbach et al., 2018) quantifies object hallucinations in image captions by comparing generated objects to ground-truth objects. Following previous works (Huang et al., 2023; Yue et al., 2024), we randomly select 500 images from the MSCOCO dataset (Lin et al., 2014) and use CHAIR_I, CHAIR_S, and Recall as evaluation metrics. **(c) MMHAL-Bench** (Sun et al., 2023): This benchmark evaluates LVLMs beyond object hallucination and contains eight question types: object attributes, adversarial objects, comparisons, counting, spatial relations, environment, holistic description, and others. We evaluate the hallucination rate and response informativeness using GPT-4.

Model	LLaVA-1.5		InstructBLIP		Qwen-VL	
Method	Accuracy ↑	F1 Score ↑	Accuracy ↑	F1 Score ↑	Accuracy ↑	F1 Score ↑
Vanilla	79.8	79.4	76.3	78.0	83.5	81.2
VCD	82.3	83.4	80.1	81.0	84.5	83.3
OPERA	84.2	83.7	79.6	80.9	84.3	82.6
VTI	**86.5**	**85.9**	**81.8**	**83.2**	**85.2**	**84.1**

Table 1: POPE hallucination evaluation results on three different LVLMs. We report the average F1-score and accuracy averaged across three sub-tasks. The complete table can be found in Appendix B.

Implementation Details. We evaluate the effectiveness of our model on three mainstream large vision-language models, including InstructBLIP (Dai et al., 2023), LLaVA 1.5 (Liu et al., 2023b) and Qwen-VL (Bai et al., 2023b) with beam search as the default decoding strategy (denoted as Regular). We also compare our model with state-of-the-art baseline methods: OPERA (Huang et al., 2023) and VCD (Leng et al., 2023b). These methods focus on mitigating object hallucinations by improving the decoding strategy. We perform a grid search for the strength of vision and text vectors where $\alpha, \beta \in \{0.1, 0.2, 0.3, 0.4, 0.5, 0.6, 0.7, 0.8, 0.9, 1.0\}$. For baseline methods, we followed the settings in their papers and released code to ensure a fair comparison. More details are provided in the Appendix A.

5.2 Experimental Results

Results on POPE. We begin with the most extensively used benchmark for object hallucination. In Table 1, we compare various decoding-based hallucination mitigation methods on the POPE benchmark (Li et al., 2023c), where "Vanilla" stands for the original model. Obviously, VTI outperforms the regular decoding strategies across all LVLMs consistently, resulting in the best accuracy and F1 score. In addition, VTI surpasses state-of-the-art contrastive decoding methods, demonstrating its effectiveness in mitigating object hallucinations. Notice that we average three different sub-tasks in POPE, and the comprehensive results can be found in Appendix B.

Results on Open-ended Generation with CHAIR Evaluation. Beyond the "Yes-or-No" discriminative evaluations on POPE, we validate our model on open-ended caption generation using the CHAIR benchmark (Rohrbach et al., 2018). The results in Table 2 demonstrate consistent improvement over the compared methods. Remarkably, visual shifting and textual shifting demonstrate effectiveness on different assessment dimensions: visual shifting is more effective in reducing CHAIR_I that calculates on image-level, while textual shifting is more effective in reducing CHAIR_s that calculates on sentence-level. Combining them (VTI, the last row) helps incorporate their benefits and effectively reduces object hallucinations in generated captions, as evidenced by lower CHAIR_S and CHAIR_I scores. In addition, VTI also maintains the comprehensiveness of the generated captions, as indicated by higher recall scores.

Results on MMHAL-Bench. To extensively test our method on various vision tasks, we benchmark VTI on the MMHAL dataset with the evaluations of eight different hallucination types. Comparison with existing methods are shown in Table 3, and a fine-grained ablation is presented in Figure 4, VTI achieves a much higher score (corresponds to less hallucination) across all categories. This underscores its effectiveness in addressing a broader range of multimodal hallucination challenges beyond objects. We also observe that textual and visual shifting are complementary. Visual shifting performs better on vision-centric tasks such as recognizing and comparing attributes of objects. In contrast, textual shifting is good at reducing hallucination of textual-centric tasks such as answering adversarial questions and counting, where relatively more complex language reasoning is required.

5.3 Analysis

Can visual shifting improve feature stability? As we discussed in Section 3, simply averaging vision embeddings across multiple perturbed images can reduce hallucination. VTI serves as a "soft" alternative to the naive averaging, and it remains unclear whether the algorithm indeed improve feature stability. To show this, we apply various types of pertubations to images, including random mask, Gaussian blur, random noise, random brightness adjustment, and random elastic transform. For

Model	Method	$\text{CHAIR}_S \downarrow$	$\text{CHAIR}_I \downarrow$	Recall ↑	Avg. Len
LLaVA1.5	Vanilla	51.0	15.2	75.2	102.2
	DOLA	57.0	15.9	78.2	97.5
	VCD	51.0	14.9	77.2	101.9
	OPERA	47.0	14.6	78.5	95.3
	Vision only	43.2	12.7	**78.6**	93.4
	Text only	41.0	12.9	78.3	92.2
	VTI	**35.8**	**11.1**	76.8	93.8
InstructBLIP	Vanilla	54.0	18.1	71.1	115.3
	DOLA	60.0	20.1	71.5	110.8
	VCD	57.0	17.0	72.1	112.1
	OPERA	54.0	12.8	69.8	93.6
	Vision only	49.1	12.1	**72.5**	104.2
	Text only	48.7	14.2	72.1	98.7
	VTI	**43.4**	**11.8**	70.1	105.8

Table 2: CHAIR hallucination evaluation results with max new tokens set to 512. Smaller CHAIR corresponds to less hallucination, and higher recall is better. We bold the best results and underline the second-best results. VTIand its variations consistently have the lowest hallucination rate with similar recall.

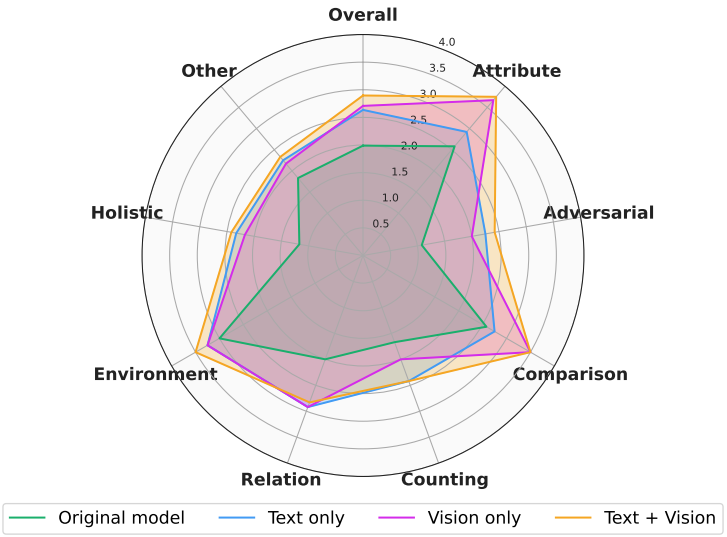

Figure 4: Detailed performance of different models on the eight categories in MMHAL-BENCH (Sun et al., 2023), where "Overall" indicates the averaged performance across all categories. A higher score indicates that the generated response contains fewer hallucinations and more information.

each of the settings, we compute the feature variance (across 100 perturbations) and average across different features as the metric of feature stability. We then compare the feature stability with/without applying VTI in Figure 5. As expected, the vision features obtained from the model with vision intervention exhibit lower variance and better stability, suggesting the effectiveness of the vision direction in smoothing out the vision features.

Textual intervention increases attention dependency toward images. It has been observed that LVLMs can occasionally disregard input image's information but treat the next-token prediction as a purely text-based continuation task (Zhu et al., 2024). Text intervention, by pushing the latent space features to the non-hallucination direction, implicitly reduces such text-biased hallucinations. Figure 6 illustrates that textual intervention is able to reduce average attention from generated text to text while increasing attention to vision tokens, suggesting higher reliance on the image when generating text.

Method	Average score ↑	Hallucination rate ↓	Attribute	Adversarial	Comparison	Counting	Relation	Environment	Holistic	Other
Vanilla	1.99	0.62	2.58	1.08	2.58	1.67	2.00	3.00	1.17	1.83
VCD	2.69	0.58	3.25	2.17	3.00	**2.42**	2.58	3.25	**2.42**	**2.42**
OPERA	2.64	0.59	2.92	2.25	2.75	**2.42**	**2.92**	3.25	2.33	2.25
VTI	**2.90**	**0.51**	**3.75**	**2.42**	**3.50**	**2.42**	2.83	**3.5**	**2.42**	2.33

Table 3: Results on MMHAL-Bench (Sun et al., 2023) with LLaVA-1.5. Our proposed method significantly reduces hallucinations in different categories.

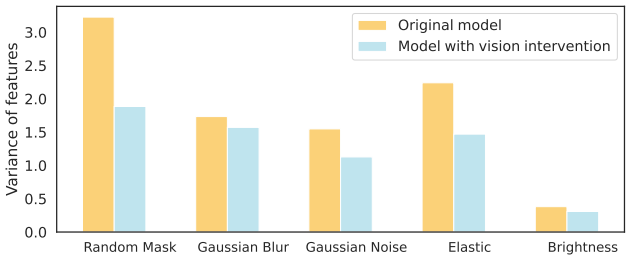

Figure 5: Feature stability is improved across different types of image corruptions with vision intervention.

Combining visual and textual intervention can enhance the level of detail in generations. A straightforward, though unremarkable, approach to reducing hallucinations is to generate less content. However, as illustrated in Figure 6, combining visual and textual interventions offers the advantage of achieving similar hallucination reduction without the need to shorten the generation length.

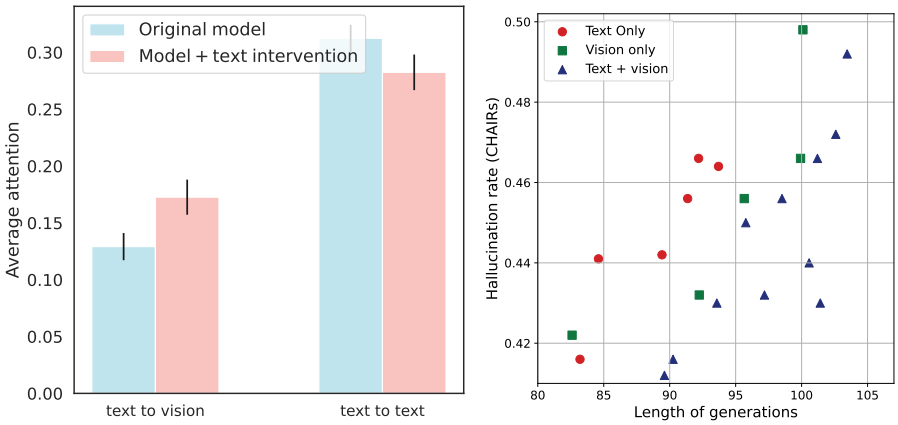

Figure 6: (Left) Textual intervention reduces the self-attention from text to text tokens and increases the self-attention to the vision tokens. (Right) Combining vision and text intervention can achieve similar hallucination rates but with longer generations.

Why is visual intervention more effective than simple vision feature averaging? In Section 3, we illustrate the effectiveness of averaging features to mitigate hallucination, however, adding random noise to the input images and averaging the corresponding features may result in a loss of information. As we demonstrated in Figure 8, performing linear probing on the simple averaged features results in only around 62% classification accuracy while applying visual intervention with different strength α resulting in improvement of visual feature stability (expressed in lower feature variance) without significantly hurting the probing accuracy, suggesting better information preservation.

Ablation of α and β. Eventually, we study the influence of vector strength applied on hidden states. Figure 8 presents the results of an ablation study on α and β, which controls the strength of visual and textual intervention, respectively. Figure 8 illustrates that $\alpha = \beta = 0$, implying no intervention, results in suboptimal performance on CHAIRs. As α and β increase, improvements in the hallucination rate are observed, highlighting the effectiveness of the visual and textual intervention.

6 Conclusion

In conclusion, our exploration into mitigating object hallucinations in LVLMs through latent space steering has yielded promising results. By implementing visual and textual intervention, we have significantly reduced hallucinations without compromising the models' ability to generate detailed and contextually accurate outputs. Our findings underline the importance of robust feature representation and its pivotal role in enhancing model reliability. As LVLMs continue to evolve, we believe the strategies outlined in this paper will serve as foundational steps toward creating more accurate, trustworthy, and efficient systems, fostering broader applicability in real-world scenarios. We are optimistic that future advancements will build on these insights, bridging the gap between human-like understanding and machine-generated interpretations.

Ethic and Reproducibility Statement

We propose the visual and textual intervention method to address hallucination issues in LVLMs, thereby enhancing their safety and reliability within the community. Additionally, the datasets utilized for inferring and evaluating our method are publicly accessible, promoting transparency and reproducibility in our research. Furthermore, we will make our code available to the public once accepted, ensuring it is convenient for researchers and practitioners to access and implement.

References

Vedika Agarwal, Rakshith Shetty, and Mario Fritz. Towards causal vqa: Revealing and reducing spurious correlations by invariant and covariant semantic editing. In *Proceedings of the IEEE/CVF Conference on Computer Vision and Pattern Recognition*, pp. 9690–9698, 2020.

Aishwarya Agrawal, Dhruv Batra, and Devi Parikh. Analyzing the behavior of visual question answering models. *arXiv preprint arXiv:1606.07356*, 2016.

Jinze Bai, Shuai Bai, Yunfei Chu, Zeyu Cui, Kai Dang, Xiaodong Deng, Yang Fan, Wenbin Ge, Yu Han, Fei Huang, et al. Qwen technical report. *arXiv preprint arXiv:2309.16609*, 2023a.

Jinze Bai, Shuai Bai, Shusheng Yang, Shijie Wang, Sinan Tan, Peng Wang, Junyang Lin, Chang Zhou, and Jingren Zhou. Qwen-vl: A frontier large vision-language model with versatile abilities. *arXiv preprint arXiv:2308.12966*, 2023b.

Tom Brown, Benjamin Mann, Nick Ryder, Melanie Subbiah, Jared D Kaplan, Prafulla Dhariwal, Arvind Neelakantan, Pranav Shyam, Girish Sastry, Amanda Askell, et al. Language models are few-shot learners. *Advances in neural information processing systems*, 33:1877–1901, 2020.

Zouying Cao, Yifei Yang, and Hai Zhao. Nothing in excess: Mitigating the exaggerated safety for llms via safety-conscious activation steering. *arXiv preprint arXiv:2408.11491*, 2024.

Wei-Lin Chiang, Zhuohan Li, Zi Lin, Ying Sheng, Zhanghao Wu, Hao Zhang, Lianmin Zheng, Siyuan Zhuang, Yonghao Zhuang, Joseph E. Gonzalez, Ion Stoica, and Eric P. Xing. Vicuna: An open-source chatbot impressing gpt-4 with 90%* chatgpt quality, March 2023. URL `https://lmsys.org/blog/2023-03-30-vicuna/`.

Aakanksha Chowdhery, Sharan Narang, Jacob Devlin, Maarten Bosma, Gaurav Mishra, Adam Roberts, Paul Barham, Hyung Won Chung, Charles Sutton, Sebastian Gehrmann, et al. Palm: Scaling language modeling with pathways. *arXiv preprint arXiv:2204.02311*, 2022.

Wenliang Dai, Junnan Li, Dongxu Li, Anthony Meng Huat Tiong, Junqi Zhao, Weisheng Wang, Boyang Li, Pascale Fung, and Steven Hoi. Instructblip: Towards general-purpose vision-language models with instruction tuning. *arXiv preprint arXiv:2306.04387*, 2023.

Ailin Deng, Zhirui Chen, and Bryan Hooi. Seeing is believing: Mitigating hallucination in large vision-language models via clip-guided decoding. *arXiv preprint arXiv:2402.15300*, 2024.

Alessandro Favero, Luca Zancato, Matthew Trager, Siddharth Choudhary, Pramuditha Perera, Alessandro Achille, Ashwin Swaminathan, and Stefano Soatto. Multi-modal hallucination control by visual information grounding. *arXiv preprint arXiv:2403.14003*, 2024.

Fabrizio Gilardi, Meysam Alizadeh, and Maël Kubli. Chatgpt outperforms crowd-workers for text-annotation tasks. *arXiv preprint arXiv:2303.15056*, 2023.

Tao Gong, Chengqi Lyu, Shilong Zhang, Yudong Wang, Miao Zheng, Qian Zhao, Kuikun Liu, Wenwei Zhang, Ping Luo, and Kai Chen. Multimodal-gpt: A vision and language model for dialogue with humans. *arXiv preprint arXiv:2305.04790*, 2023.

Yash Goyal, Tejas Khot, Douglas Summers-Stay, Dhruv Batra, and Devi Parikh. Making the v in vqa matter: Elevating the role of image understanding in visual question answering. In *Proceedings of the IEEE conference on computer vision and pattern recognition*, pp. 6904–6913, 2017.

Anisha Gunjal, Jihan Yin, and Erhan Bas. Detecting and preventing hallucinations in large vision language models. *arXiv preprint arXiv:2308.06394*, 2023.

Yudong Han, Liqiang Nie, Jianhua Yin, Jianlong Wu, and Yan Yan. Visual perturbation-aware collaborative learning for overcoming the language prior problem. *arXiv preprint arXiv:2207.11850*, 2022.

Qidong Huang, Xiaoyi Dong, Pan Zhang, Bin Wang, Conghui He, Jiaqi Wang, Dahua Lin, Weiming Zhang, and Nenghai Yu. Opera: Alleviating hallucination in multi-modal large language models via over-trust penalty and retrospection-allocation. *arXiv preprint arXiv:2311.17911*, 2023.

Ziwei Ji, Nayeon Lee, Rita Frieske, Tiezheng Yu, Dan Su, Yan Xu, Etsuko Ishii, Ye Jin Bang, Andrea Madotto, and Pascale Fung. Survey of hallucination in natural language generation. *ACM Computing Surveys*, 55(12):1–38, 2023.

Junho Kim, Yeon Ju Kim, and Yong Man Ro. What if...?: Counterfactual inception to mitigate hallucination effects in large multimodal models. *arXiv preprint arXiv:2403.13513*, 2024.

Xin Lai, Zhuotao Tian, Yukang Chen, Yanwei Li, Yuhui Yuan, Shu Liu, and Jiaya Jia. Lisa: Reasoning segmentation via large language model. In *Proceedings of the IEEE/CVF Conference on Computer Vision and Pattern Recognition*, pp. 9579–9589, 2024.

Jusung Lee, Sungguk Cha, Younghyun Lee, and Cheoljong Yang. Visual question answering instruction: Unlocking multimodal large language model to domain-specific visual multitasks. *arXiv preprint arXiv:2402.08360*, 2024.

Seongyun Lee, Sue Hyun Park, Yongrae Jo, and Minjoon Seo. Volcano: mitigating multimodal hallucination through self-feedback guided revision. *arXiv preprint arXiv:2311.07362*, 2023.

Sicong Leng, Hang Zhang, Guanzheng Chen, Xin Li, Shijian Lu, Chunyan Miao, and Lidong Bing. Mitigating object hallucinations in large vision-language models through visual contrastive decoding. *arXiv preprint arXiv:2311.16922*, 2023a.

Sicong Leng, Hang Zhang, Guanzheng Chen, Xin Li, Shijian Lu, Chunyan Miao, and Lidong Bing. Mitigating object hallucinations in large vision-language models through visual contrastive decoding. *arXiv preprint arXiv:2311.16922*, 2023b.

Bo Li, Yuanhan Zhang, Liangyu Chen, Jinghao Wang, Jingkang Yang, and Ziwei Liu. Otter: A multi-modal model with in-context instruction tuning. *arXiv preprint arXiv:2305.03726*, 2023a.

Junnan Li, Dongxu Li, Caiming Xiong, and Steven Hoi. Blip: Bootstrapping language-image pre-training for unified vision-language understanding and generation. In *International Conference on Machine Learning*, pp. 12888–12900. PMLR, 2022.

Junnan Li, Dongxu Li, Silvio Savarese, and Steven Hoi. Blip-2: Bootstrapping language-image pre-training with frozen image encoders and large language models. *arXiv preprint arXiv:2301.12597*, 2023b.

Liunian Harold Li, Mark Yatskar, Da Yin, Cho-Jui Hsieh, and Kai-Wei Chang. Visualbert: A simple and performant baseline for vision and language. *arXiv preprint arXiv:1908.03557*, 2019.

Yifan Li, Yifan Du, Kun Zhou, Jinpeng Wang, Wayne Xin Zhao, and Ji-Rong Wen. Evaluating object hallucination in large vision-language models. *arXiv preprint arXiv:2305.10355*, 2023c.

Tsung-Yi Lin, Michael Maire, Serge Belongie, James Hays, Pietro Perona, Deva Ramanan, Piotr Dollár, and C Lawrence Zitnick. Microsoft coco: Common objects in context. In *Computer Vision–ECCV 2014: 13th European Conference, Zurich, Switzerland, September 6-12, 2014, Proceedings, Part V 13*, pp. 740–755. Springer, 2014.

Fuxiao Liu, Kevin Lin, Linjie Li, Jianfeng Wang, Yaser Yacoob, and Lijuan Wang. Mitigating hallucination in large multi-modal models via robust instruction tuning. *arXiv preprint arXiv:2306.14565*, 2023a.

Hanchao Liu, Wenyuan Xue, Yifei Chen, Dapeng Chen, Xiutian Zhao, Ke Wang, Liping Hou, Rongjun Li, and Wei Peng. A survey on hallucination in large vision-language models. *arXiv preprint arXiv:2402.00253*, 2024a.

Haotian Liu, Chunyuan Li, Qingyang Wu, and Yong Jae Lee. Visual instruction tuning. *arXiv preprint arXiv:2304.08485*, 2023b.

Sheng Liu, Haotian Ye, Lei Xing, and James Y Zou. In-context vectors: Making in context learning more effective and controllable through latent space steering. In *Forty-first International Conference on Machine Learning*.

Sheng Liu, Oscar Pastor-Serrano, Yizheng Chen, Matthew Gopaulchan, Weixing Liang, Mark Buyyounouski, Erqi Pollom, Quynh-Thu Le, Michael Gensheimer, Peng Dong, et al. Automated radiotherapy treatment planning guided by gpt-4vision. *arXiv preprint arXiv:2406.15609*, 2024b.

Holy Lovenia, Wenliang Dai, Samuel Cahyawijaya, Ziwei Ji, and Pascale Fung. Negative object presence evaluation (nope) to measure object hallucination in vision-language models. *arXiv preprint arXiv:2310.05338*, 2023.

Jinqi Luo, Tianjiao Ding, Kwan Ho Ryan Chan, Darshan Thaker, Aditya Chattopadhyay, Chris Callison-Burch, and René Vidal. Pace: Parsimonious concept engineering for large language models. *arXiv preprint arXiv:2406.04331*, 2024.

Alec Radford, Jong Wook Kim, Chris Hallacy, Aditya Ramesh, Gabriel Goh, Sandhini Agarwal, Girish Sastry, Amanda Askell, Pamela Mishkin, Jack Clark, et al. Learning transferable visual models from natural language supervision. In *International conference on machine learning*, pp. 8748–8763. PMLR, 2021.

Colin Raffel, Noam Shazeer, Adam Roberts, Katherine Lee, Sharan Narang, Michael Matena, Yanqi Zhou, Wei Li, and Peter J Liu. Exploring the limits of transfer learning with a unified text-to-text transformer. *The Journal of Machine Learning Research*, 21(1):5485–5551, 2020.

Anna Rohrbach, Lisa Anne Hendricks, Kaylee Burns, Trevor Darrell, and Kate Saenko. Object hallucination in image captioning. *arXiv preprint arXiv:1809.02156*, 2018.

Weijia Shi, Sewon Min, Michihiro Yasunaga, Minjoon Seo, Rich James, Mike Lewis, Luke Zettlemoyer, and Wen-tau Yih. Replug: Retrieval-augmented black-box language models. *arXiv preprint arXiv:2301.12652*, 2023.

Chen Sun, Austin Myers, Carl Vondrick, Kevin Murphy, and Cordelia Schmid. Videobert: A joint model for video and language representation learning. In *Proceedings of the IEEE/CVF international conference on computer vision*, pp. 7464–7473, 2019.

Zhiqing Sun, Sheng Shen, Shengcao Cao, Haotian Liu, Chunyuan Li, Yikang Shen, Chuang Gan, Liang-Yan Gui, Yu-Xiong Wang, Yiming Yang, et al. Aligning large multimodal models with factually augmented rlhf. *arXiv preprint arXiv:2309.14525*, 2023.

Rohan Taori, Ishaan Gulrajani, Tianyi Zhang, Yann Dubois, Xuechen Li, Carlos Guestrin, Percy Liang, and Tatsunori B. Hashimoto. Stanford alpaca: An instruction-following llama model, 2023.

Yi Tay, Mostafa Dehghani, Vinh Q Tran, Xavier Garcia, Jason Wei, Xuezhi Wang, Hyung Won Chung, Dara Bahri, Tal Schuster, Steven Zheng, et al. Ul2: Unifying language learning paradigms. In *The Eleventh International Conference on Learning Representations*, 2022.

Hugo Touvron, Thibaut Lavril, Gautier Izacard, Xavier Martinet, Marie-Anne Lachaux, Timothée Lacroix, Baptiste Rozière, Naman Goyal, Eric Hambro, Faisal Azhar, et al. Llama: Open and efficient foundation language models. *arXiv preprint arXiv:2302.13971*, 2023.

David Wan, Jaemin Cho, Elias Stengel-Eskin, and Mohit Bansal. Contrastive region guidance: Improving grounding in vision-language models without training. *arXiv preprint arXiv:2403.02325*, 2024.

Haibo Wang, Chenghang Lai, Yixuan Sun, and Weifeng Ge. Weakly supervised gaussian contrastive grounding with large multimodal models for video question answering. *arXiv preprint arXiv:2401.10711*, 2024a.

Jianfeng Wang, Zhengyuan Yang, Xiaowei Hu, Linjie Li, Kevin Lin, Zhe Gan, Zicheng Liu, Ce Liu, and Lijuan Wang. Git: A generative image-to-text transformer for vision and language. *arXiv preprint arXiv:2205.14100*, 2022.

Junyang Wang, Yiyang Zhou, Guohai Xu, Pengcheng Shi, Chenlin Zhao, Haiyang Xu, Qinghao Ye, Ming Yan, Ji Zhang, Jihua Zhu, et al. Evaluation and analysis of hallucination in large vision-language models. *arXiv preprint arXiv:2308.15126*, 2023a.

Teng Wang, Jinrui Zhang, Junjie Fei, Yixiao Ge, Hao Zheng, Yunlong Tang, Zhe Li, Mingqi Gao, Shanshan Zhao, Ying Shan, et al. Caption anything: Interactive image description with diverse multimodal controls. *arXiv preprint arXiv:2305.02677*, 2023b.

Xintong Wang, Jingheng Pan, Liang Ding, and Chris Biemann. Mitigating hallucinations in large vision-language models with instruction contrastive decoding. *arXiv preprint arXiv:2403.18715*, 2024b.

Yike Wu, Yu Zhao, Shiwan Zhao, Ying Zhang, Xiaojie Yuan, Guoqing Zhao, and Ning Jiang. Overcoming language priors in visual question answering via distinguishing superficially similar instances. *arXiv preprint arXiv:2209.08529*, 2022.

Dingchen Yang, Bowen Cao, Guang Chen, and Changjun Jiang. Pensieve: Retrospect-then-compare mitigates visual hallucination. *arXiv preprint arXiv:2403.14401*, 2024.

Qinghao Ye, Haiyang Xu, Guohai Xu, Jiabo Ye, Ming Yan, Yiyang Zhou, Junyang Wang, Anwen Hu, Pengcheng Shi, Yaya Shi, Chenliang Li, Yuanhong Xu, Hehong Chen, Junfeng Tian, Qian Qi, Ji Zhang, and Fei Huang. mplug-owl: Modularization empowers large language models with multimodality. *arXiv preprint arXiv:2304.14178*, 2023.

Shukang Yin, Chaoyou Fu, Sirui Zhao, Tong Xu, Hao Wang, Dianbo Sui, Yunhang Shen, Ke Li, Xing Sun, and Enhong Chen. Woodpecker: Hallucination correction for multimodal large language models. *arXiv preprint arXiv:2310.16045*, 2023.

Zihao Yue, Liang Zhang, and Qin Jin. Less is more: Mitigating multimodal hallucination from an eos decision perspective. *arXiv preprint arXiv:2402.14545*, 2024.

Bohan Zhai, Shijia Yang, Xiangchen Zhao, Chenfeng Xu, Sheng Shen, Dongdi Zhao, Kurt Keutzer, Manling Li, Tan Yan, and Xiangjun Fan. Halle-switch: Rethinking and controlling object existence hallucinations in large vision language models for detailed caption. *arXiv preprint arXiv:2310.01779*, 2023.

Xiaoman Zhang, Chaoyi Wu, Ziheng Zhao, Weixiong Lin, Ya Zhang, Yanfeng Wang, and Weidi Xie. Pmc-vqa: Visual instruction tuning for medical visual question answering. *arXiv preprint arXiv:2305.10415*, 2023a.

Yi-Fan Zhang, Weichen Yu, Qingsong Wen, Xue Wang, Zhang Zhang, Liang Wang, Rong Jin, and Tieniu Tan. Debiasing large visual language models. *arXiv preprint arXiv:2403.05262*, 2024.

Yue Zhang, Yafu Li, Leyang Cui, Deng Cai, Lemao Liu, Tingchen Fu, Xinting Huang, Enbo Zhao, Yu Zhang, Yulong Chen, et al. Siren's song in the ai ocean: A survey on hallucination in large language models. *arXiv preprint arXiv:2309.01219*, 2023b.

Linxi Zhao, Yihe Deng, Weitong Zhang, and Quanquan Gu. Mitigating object hallucination in large vision-language models via classifier-free guidance. *arXiv preprint arXiv:2402.08680*, 2024.

Zhiyuan Zhao, Bin Wang, Linke Ouyang, Xiaoyi Dong, Jiaqi Wang, and Conghui He. Beyond hallucinations: Enhancing lvlms through hallucination-aware direct preference optimization. *arXiv preprint arXiv:2311.16839*, 2023.

Ren Zhibo, Wang Huizhen, Zhu Muhua, Wang Yichao, Xiao Tong, and Zhu Jingbo. Overcoming language priors with counterfactual inference for visual question answering. In *Proceedings of the 22nd Chinese National Conference on Computational Linguistics*, pp. 600–610, 2023.

Yiyang Zhou, Chenhang Cui, Jaehong Yoon, Linjun Zhang, Zhun Deng, Chelsea Finn, Mohit Bansal, and Huaxiu Yao. Analyzing and mitigating object hallucination in large vision-language models. *arXiv preprint arXiv:2310.00754*, 2023.

Deyao Zhu, Jun Chen, Xiaoqian Shen, Xiang Li, and Mohamed Elhoseiny. Minigpt-4: Enhancing vision-language understanding with advanced large language models. *arXiv preprint arXiv:2304.10592*, 2023.

Lanyun Zhu, Deyi Ji, Tianrun Chen, Peng Xu, Jieping Ye, and Jun Liu. Ibd: Alleviating hallucinations in large vision-language models via image-biased decoding. *arXiv preprint arXiv:2402.18476*, 2024.

Andy Zou, Long Phan, Sarah Chen, James Campbell, Phillip Guo, Richard Ren, Alexander Pan, Xuwang Yin, Mantas Mazeika, Ann-Kathrin Dombrowski, et al. Representation engineering: A top-down approach to ai transparency. *arXiv preprint arXiv:2310.01405*, 2023.

A Detailed Experimental Settings

In all experimental setups, the mask ratio to compute visual direction is set to 0.99, and we average across 50 random masks. For experiments on CHAIR, to maintain similar lengths of generations, we set $\alpha = 0.4$ for visual intervention only, similarly $\beta = 0.4$ for textual intervention only. For VTI , $\alpha = 0.2$ and $\beta = 0.4$. For experiments on MMHAL-BENCH, we adopted $\alpha = 0.9$ and $\beta = 0.9$. For POPE and CHAIR, we employed nucleus sampling for decoding; For MMHAL-BENCH, we used beam search with the number of beams set to 5 to showcase the effectiveness of our method across different decoding strategies.

POPE[1] We utilize the official benchmark from Li et al. (2023c), which includes 3,000 question-answer pairs for each of the random, popular, and adversarial settings. We use the query template 'Is there a [object] in the image?'. Here, [object] is selected randomly, from the most frequent objects in the dataset, or from objects that frequently co-occur with [object], corresponding to the random, popular, and adversarial settings respectively. We evaluate the performance based on whether the model-generated output contained the ground truth ('Yes' or 'No') using accuracy, precision, recall, and average F1-score.

CHAIR[2] We select 500 random images from the COCO Lin et al. (2014) validation set and generate the output using the query "Please Describe this image in detail.". Due to the computational complexity, we restrict the *max new tokens* to 64. Following the M3ID Favero et al. (2024), we report two assessment metrics, CHAIR_s and CHAIR_i, which calculate the hallucination ratio per sentence and instance as follows:

$$\text{CHAIR}_s = \frac{|\{\text{sentences with hallucinated objects}\}|}{|\{\text{all sentences}\}|}, \text{CHAIR}_i = \frac{|\{\text{hallucinated objects}\}|}{|\{\text{all objects mentioned}\}|}. \quad (5)$$

[1] https://github.com/RUCAIBox/POPE

[2] https://github.com/LisaAnne/Hallucination

MMHAL-Bench[3] In MMHAL-Bench dataset, 96 image-question pairs, ranging in 8 question categories × 12 object topics are included. The question categories are

- **Object attribute:** LVLMs incorrectly describe the visual attributes of invididual objects, such as color and shape.
- **Adversarial object:** LVLMs answers questions involving something that does not exist in the image, instead of pointing out that the referred object cannot be found.
- **Comparison:** LVLMs incorrectly compare the attributes of multiple objects.
- **Counting:** LVLMs fail to count the number of the named objects.
- **Spatial relation:** LVLMs fail to understand the spatial relations between multiple objects in the response.
- **Environment:** LVLMs make wrong inference about the environment of the given image.
- **Holistic description:** LVLMs make false claims about contents in the given image when giving a comprehensive and detailed description of the whole image.
- **Others:** LVLMs fail to recognize the text or icons, or incorrectly reason based on the observed visual information

Following Sun et al. (2023), we use GPT-4 to evaluate different methods on MMHAL-BENCH and to analyze and rate responses. Prompts we used for MMHAL-BENCH evaluation can be found in (Sun et al., 2023). The rating scales are

- 6, very informative with good analysis or reasoning, no hallucination
- 5, very informative, no hallucination
- 4, somewhat informative, no hallucination
- 3, not informative, no hallucination
- 2, very informative, with hallucination
- 1, somewhat informative, with hallucination
- 0, not informative, with hallucination

and if the rating < 3, the generation is considered with hallucination.

B Additional Experiment Results

B.1 Detailed Results on POPE

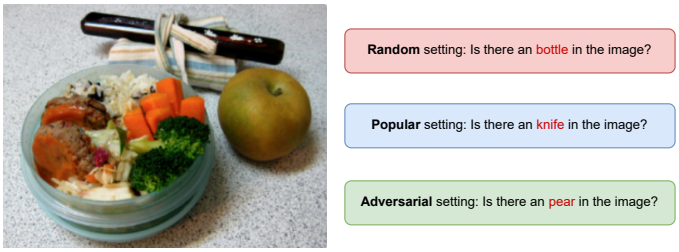

Figure 7: Example questions in different settings of the POPE dataset

We present the detailed performance on POPE in Table 4. VTI exhibits significant performance improvement with LLaVA-1.5, InstructBLIP, and Qwen-VL. These results underscore the effectiveness of VTI in mitigating object hallucination.

[3]https://huggingface.co/datasets/Shengcao1006/MMHal-Bench

Setting	Model	Decoding	Accuracy	Precision	Recall	F1 Score
Random	LLaVA1.5	Regular	83.49	88.84	76.76	82.36
		OPERA	87.53	**94.52**	79.80	86.53
		VCD	86.84	87.15	**86.68**	86.91
		VTI	**89.50**	94.38	84.00	**88.89**
	InstructBLIP	Regular	80.42	78.93	83.21	81.01
		OPERA	85.07	88.39	80.73	84.39
		VCD	84.11	84.20	85.36	84.78
		VTI	**86.37**	**88.83**	**85.68**	**87.22**
	Qwen-VL	Regular	84.33	95.98	71.67	82.06
		OPERA	85.13	**95.54**	74.13	83.48
		VCD	85.53	95.17	74.87	83.81
		VTI	**86.73**	93.67	**78.80**	**85.59**
Popular	LLaVA1.5	Regular	79.98	82.47	76.76	79.51
		OPERA	84.21	88.00	79.80	83.70
		VCD	82.65	87.15	80.59	83.74
		VTI	**87.36**	**91.61**	**82.27**	**86.69**
	InstructBLIP	Regular	76.09	73.22	82.94	77.78
		OPERA	78.33	73.85	87.73	80.19
		VCD	79.94	77.84	83.33	80.49
		VTI	**81.86**	**80.17**	**85.68**	**82.83**
	Qwen-VL	Regular	84.17	96.13	71.20	81.81
		OPERA	84.73	**96.52**	73.13	83.21
		VCD	85.63	94.28	75.87	84.08
		VTI	**85.67**	92.06	**78.06**	**84.48**
Adversarial	LLaVA1.5	Regular	76.03	76.11	76.80	76.45
		OPERA	80.88	82.16	79.76	80.94
		VCD	77.31	73.43	**86.47**	79.42
		VTI	**82.57**	**84.33**	80.01	**82.11**
	InstructBLIP	Regular	72.37	68.78	83.06	75.24
		OPERA	75.50	70.49	**87.73**	78.17
		VCD	76.32	73.24	84.08	78.29
		VTI	**77.29**	**74.09**	85.67	**79.46**
	Qwen-VL	Regular	81.93	91.30	70.60	79.62
		OPERA	82.93	**91.15**	73.31	81.26
		VCD	82.19	90.14	75.53	**82.19**
		VTI	**83.13**	88.20	**77.67**	82.16

Table 4: Experimental results on POPE (Li et al., 2023c).

B.2 Detailed Results on MMHAL-Bench

We present the detailed performance on MMHAL-Bench in Table 3presents the detailed performance metrics on MMHAL-Bench. VTI demonstrates substantial improvements across various tasks, consistently outperforming both VCD and OPERA in all question categories except for the 'Other' category. These results highlight the effectiveness of VTI in reducing hallucinations beyond object-specific errors, reinforcing its potential to enhance LVLMs' accuracy in interpreting and analyzing visual content comprehensively.

B.3 More results on analysis

In this section, we provide additional figures (Figure 8) on the analysis section in the main text.

C Examples for computing the textual directions.

To generate hallucinated captions for our experiments, we curated a training set of 50 examples using the methodology outlined in (Zhou et al., 2023). Specifically, we leveraged GPT-3.5's in-context

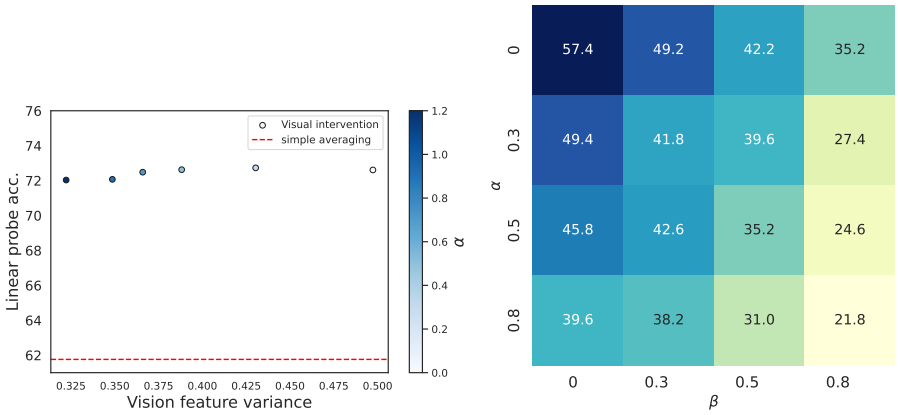

Figure 8: (Left) Trade-off between robustness and information preservation. Visual shifting improves feature robustness while preserving information. α controls the strength of the shifting. (Right) Ablation study on α and β.

Method	**Hallucination Rate (%)**
LLaVA-1.5	61.46
VTI (PCA dim = 1)	51.04
VTI (PCA dim = 3)	51.04
VTI (simple average)	57.96

Table 5: VTI performance with different PCA dimensions. Experiments are conducted on MMHAL-Bench.

learning capabilities to automatically generate hallucinatory data for refinement. First, GPT-3.5 was prompted to produce a list of objects that frequently co-occur with the ones mentioned in a given description. Then, using LLaVA-1.5, we generated descriptions for the 50 training images, incorporating a randomly selected word from the "co-occurring objects" list and another from the "uncertain objects" list. This process allowed us to create a rich dataset of hallucinated captions. For further details on the prompts, refer to (Zhou et al., 2023). Figure 9 shows the example of a generated caption.

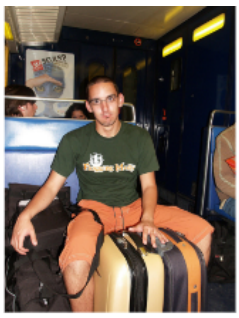

Original Caption: The image shows a young man sitting on a pile of luggage while traveling on public transportation, likely a passenger train or a bus. He has a puzzled look on his face as he tries to manage his belongings on this crowded journey.\nThere are multiple suitcases, a handbag, and a backpack nearby, indicating that the man has a considerable amount of luggage with him. Apart from the man sitting on his luggage, there are a few other people in the scene as well, some sitting on benches while others stand in the space. The two benches available are located on either side of the man sitting with his luggage. Additionally, there are handbags placed on the floor in the same area, suggesting that other passengers also have their belongings with them.

Generated hallucinated Caption: The image shows a young man with a puzzled look on his face as he tries to manage his multiple suitcases, handbag, and backpack while sitting on a pile of luggage during a crowded journey on public transportation. Other passengers are seen with their own handbags and belongings nearby. One of the passengers is seen holding a water bottle, while it is uncertain what the man in front of the young man is doing or why he is smiling.

Figure 9: Illustration of the generated hallucinated captions for textual direction computing.